United States Department of Agriculture

Forest Service

Percent Impervious Landcover Modeling: Analyzing the Impacts of Model Types, Calibration Methods, and Ecoregions

October 2013

RSAC-10025-RPT1

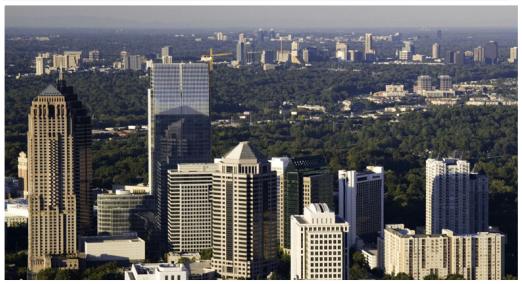

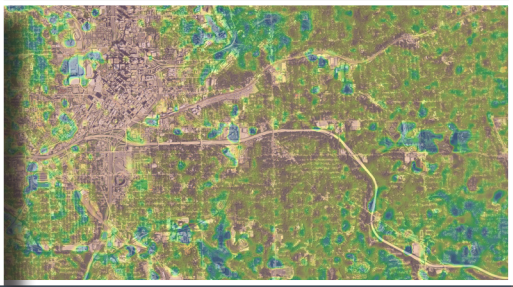

Abstract

Percent impervious landcover maps serve as valuable tools for understanding urban growth patterns and monitoring environmental and social impacts. Presently, these maps are updated about every 5 years as part of the National Land Cover Database (NLCD). More frequent updates would improve the temporal precision of our understanding of growth patterns and their impacts. Creating a consistent percent impervious landcover map on an annual basis warrants a review of the impacts of different calibration, prediction, and modeling techniques across different ecoregions. This study tests various model calibration techniques, using different model predictor variables and model types across different ecoregions, to provide a better understanding of how these methods affect model outputs. Results indicate that:

- Modeling should be performed on individual ecoregions in order to ensure maximum model performance.
- Lower bootstrapped errors were achieved when modeling percent impervious surface using a large number of calibration samples derived from an existing percent impervious landcover layer than using photo-interpreted calibration data. Deriving calibration samples from an existing map product is faster than acquiring calibration samples with photo interpretation and may be an acceptable approach when time and budget are limiting factors. However, there are many assumptions and concerns associated with this approach that need careful consideration and further investigation.
- While both Landsat and ASTER thermal data were effective for modeling percent impervious landcover within the moist-climate study areas, Landsat spectral data proved to be the best across all ecoregion types.

Results from this study suggest that creating a nationwide percent impervious landcover map on an annual basis is practical based on the wide availability of data and sufficient computing power. The next step is to gain a better understanding of the optimal automated model calibration method, model parameters, and hybridized predictor dataset.

Keywords

Percent impervious landcover, NLCD, Landsat, ASTER, MODIS, thermal remote sensing, spectral remote sensing, urbanization, random forests, support vector machine, Cubist, R, aerial photo interpretation

Authors

Ian Housman is a remote sensing specialist employed by RedCastle Resources at the Remote Sensing Applications Center (RSAC) in Salt Lake City, Utah.

Pinki Mondal is a postdoctoral research scientist at Columbia University in New York City.

Randy Hamilton is the sponsored projects group leader employed by RedCastle Resources at RSAC.

Haans Fisk is the Remote Sensing Evaluation, Application, and Training program leader at RSAC.

Andrew Lister is a research forester at the Northern Research Station in Newtown Square, Pennsylvania.

Brett Butler is a research forester at the Northern Research Station.

Dennis Jacobs is a research forester at the Southern Research Station in Asheville, North Carolina.

Tonya Lister is a research forester at the Northern Research Station.

Dumitru Salajanu is a forester and remote sensing specialist at the Southern Research Station.

Housman, I.; Mondal, P.; Hamilton, R.; Fisk, H.; Lister, A.; Butler, B.; Jacobs, D.; Lister, T.; Salajanu, D. 2013. Percent impervious landcover modeling: analyzing the impacts of model types, calibration methods, and ecoregions. RSAC-10025-RPT1. Salt Lake City, UT: U.S. Department of Agriculture, Forest Service, Remote Sensing Applications Center. 13 p.

Table of Contents

Abstract ii

Introduction 1

Study Areas 1

Methods 2

- Model Type 2
- Calibration Method Selection 3
- Predictor Types 3
- Direct Ecoregion Comparison Methods 5
- Validation Methods 5

Results 5

- Model Methods 5
- Calibration Method 5
- Predictor Data Type 6
- Direct Ecoregion Comparison 6

Discussion 7

References 10

Appendix A: Comprehensive List of Analysis Results 12

Introduction

Urban growth is an integral part of population and economic growth (Wrigley 1985). Its social, economic, and environmental impacts are pronounced. Worldwide, urbanization is on an upward trend (Cohen 2004). Developing nations have seen an increase in urban population as people move from rural areas to urban centers (Cohen 2006), while developed nations have experienced a pronounced outward expansion from urban areas as suburbanization has become more prevalent (Mieszkowski and Mills 1993). It is important to be able to monitor urban growth in a consistent manner in order to better understand the social, economic, and environmental impact of urban expansion.

Currently, there are two data products that monitor urban extent within the continental US. The National Oceanic and Atmospheric Administration's (NOAA) Defense Meteorological Satellite Program (DMSP) provides a coarse scale product with 1-km spatial resolution that depicts anthropogenic nighttime light intensity. Due to its coarse spatial resolution and worldwide coverage, this product is often used to provide large-area summaries of urban development (Ghosh and others 2010). In order to provide a more detailed depiction of urban extent, the Multi-Resolution Land Characterization (MRLC) consortium has produced a percent artificial impervious landcover map for the US using a 30- by 30-meter grid. This is part of the larger National Land Cover Database (NLCD) effort (Fry and others 2011). This product has proven effective for monitoring urban growth by using NLCD percent impervious landcover from two dates (Xian and others 2011). Unfortunately, the NLCD percent impervious landcover layer is created only every 5 years, producing a 5-year time gap in the data record of urban growth. Additionally, slight changes in NLCD percent impervious landcover mapping methods between versions introduce some inconsistency in the products, thus making direct comparisons inappropriate. Having a consistent product that is updated on an annual basis would allow for enhanced change detection capabilities, while providing greater temporal detail. Such a product would facilitate a better understanding of the spatiotemporal dynamics of urbanization.

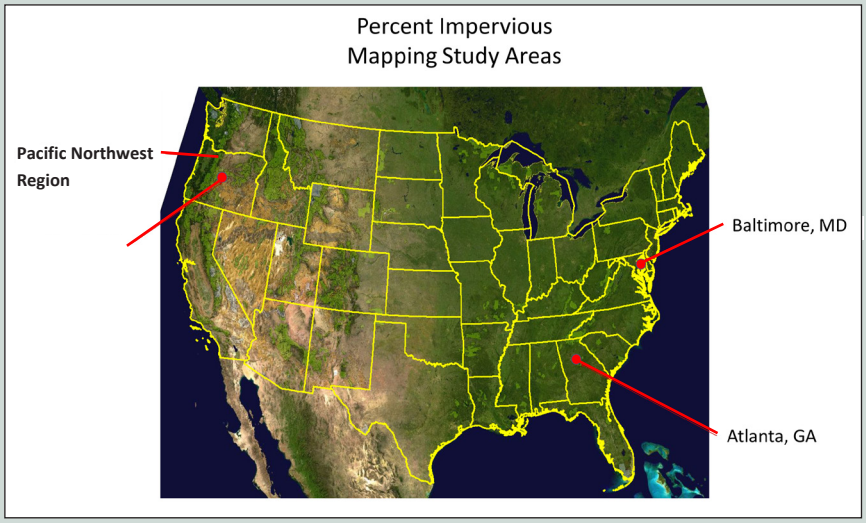

Figure 1—Map of general study area locations.

The NLCD percent impervious landcover product is modeled using a set of Landsat-based raster predictors and photo-interpreted calibration data in a Cubist™ model. All calibration data are confined to an urban extent stratum defined by a threshold on the DMSP stable anthropogenic light product (Fry and others 2011). Few studies currently seek to generalize a modeling framework, training data, and predictor information across multiple large regions. The current literature largely concentrates on comparing different predictor types or modeling methods within one region, but do not extend these concepts across different regions (Chabaeva and others 2009; Ma and others 2010; Walton 2008; Xu 2010). The key difficulty with modeling percent impervious landcover is the inconsistency in how impervious and pervious surfaces across different regions relate both spectrally and thermally. A given model may work well within a moist ecoregion but fail in an arid ecoregion. In order to create a nationwide percent impervious landcover map, an enhanced understanding of effective methods for modeling percent impervious landcover across a variety of regions is required.

This study is designed to address the current knowledge gap and provide an enhanced understanding of the effects of using different model types, predictor types, and calibration methods across different ecoregion types. The study could serve as a first step toward designing an efficient, robust workflow for modeling percent impervious landcover throughout the continental US on an annual basis.

Study Areas

Three primary study areas were chosen for this study—two moist and one arid. They are Baltimore, MD, Atlanta, GA, and Bend, OR (figure 1). The extent of each study area corresponds to the intersection of a set of ASTER thermal imagery footprints centered on the urban area of interest. (Since ASTER is a tasked sensor with an inconsistent image extent, the largest available overlap area was used.) An additional study area corresponding to the

MODIS swath that intersects the Pacific Northwest was also identified for a direct ecoregion comparison. The Baltimore and Atlanta study areas fall within the Eastern deciduous biome, which is dominated by deciduous forests. Additional common landcover types include agriculture, wetlands, and developed areas. Urban areas are generally distinct both spectrally and thermally from the surrounding, relatively cool and dark forested areas. Agricultural and other bare soil landcover categories have similar spectral and thermal properties, but vary in different ways across a single growing year. Baltimore and Atlanta were chosen due to their differing thermal and spectral characteristics, which are due to their differing latitudes and coastal proximity. Baltimore has cold winters and hot summers, while Atlanta experiences relatively mild winters with hot summers. Bend lies within an arid area in the rain shadow of the Cascades. This area is dominated by herbaceous and scrub/shrub landcover in the upland areas, while the valleys are dominated by agricultural and riparian landcover types.

Methods

To address the project objectives, a matrix of different analysis components and potential methods was developed. Combinations of the predictor layers, calibration methods, model types, and ecoregions shown in table 1 were tested. In addition, a unique test was conducted in the Pacific Northwestern region of the United States. Due to the adjacency of moist and arid ecoregions in the Pacific Northwest, it was possible to use a single MODIS swath to visually and quantitatively analyze the impacts of dividing model calibration by ecoregion.

Model Type

Three types of models were tested in this study—random forests, support vector machines and Cubist. The model types were selected due to their documented efficacy with modeling percent impervious surfaces (Walton 2008). Random forests is an ensemble regression tree classifier that has the advantage of providing error estimates and predictor variable importance level. It generally works well with weak predictors (Brieman 2001; Ghimire and others 2012). Support vector machines work by transforming a multi-dimensional feature space to a single dimension to identify a single hyperplane that separates the data. They are effective in separating non-linearly separable data using limited training data (Cortes and Vapnik 1995; Ghimire and others 2012). Support vector machines have proven effective at modeling percent impervious landcover in past studies (Walton, 2008). Cubist is a single regression tree classifier that is effective at identifying patterns in complex data, but is generally less robust than random forests and support vector machines with limited calibration data (Ghimire and others 2012). Cubist serves as the modeling method for the NLCD percent impervious landcover layer (Fry and others 2011), and was therefore included to serve as a baseline for the current state of the methods for large-area percent impervious mapping. Model source details can be found in table 2. All modeling procedures were conducted using R (R Development Core Team 2010).

Table 1—Models, predictor layers and calibration methods tested to map percent impervious landcover for each ecoregion in the study

Predictor Types	Calibration Methods	Model Types	Ecoregions
Aster Thermal	Photo interpreted (Moist only)	Cubist	Cool Moist (Baltimore)
Landsat Spectral	National Land Cover Database	Random Forest	Warm Moist (Atlanta)
Landsat Thermal		Support Vector Machine	Arid (Bend)

Table 2—Model name, R package name, and source URL for each tested model

Model	R Package Name	URL
Cubist	Cubist	http://cran.r-project.org/web/packages/Cubist/index.html
Random Forests	randomForest	http://cran.r-project.org/web/packages/randomForest/index.html
Support Vector Machine	kernlab	http://cran.r-project.org/web/packages/kernlab/index.html

Each of the chosen modeling methods has strengths and weaknesses. Model efficacy was estimated using model error metrics. Run times were also noted. Understanding the relationship between run time and model error helps provide a better understanding of which modeling method may be optimal over a large area.

Calibration Method Selection

The goal of model calibration is to fit a model to a set of calibration data that represent the variability of the attribute of interest on the landscape. Currently, there is no publicly available nationwide percent impervious landcover inventory dataset to use for model calibration. The best proxy is the NLCD percent impervious dataset itself. While this is a modeled data product, it is the only existing nationwide product. Typically, training data have been created using a sample of the landscape that was then photo-interpreted and/or ground truthed to derive a percent impervious landcover metric. This method is largely effective, but very costly and highly dependent on a consistent definition and interpretation of an impervious surface (Nowak and Greenfield 2010). If an existing modelled impervious surface product has similar definitions of percent impervious, it is possible that such data could be sampled and used as model calibration data. Huang and others (2008) demonstrated that using existing modeled landcover products to refine forest classification model calibration can increase the efficacy of the modeled output. Since their study created a thematic output using classification instead of a continuous output using regression, they were afforded the ability to pre-stratify the landscape into core forest areas. This permitted the model to only be partially reliant on the efficacy of the existing modeled output. This is not possible when modeling a continuous output, such as percent impervious surface, thus necessitating a greater reliance on the dataset that is being sampled. This key difference leaves the capabilities of regression model calibration automation largely unknown. In order to address this knowledge gap, both model calibration methods were tested within the moist region. A single ecoregion was chosen due to the cost of deriving photo-interpreted training data, and based on the assumption that the efficacy of different training methods is likely to not be ecoregion-dependent.

The photo-interpreted calibration dataset was generated using 2006 National Agriculture Imagery Program (NAIP) imagery interpreted at a stratified random sample of locations within each moist study area. The sample strata were created using a binned NLCD percent impervious landcover layer, with each bin corresponding to a 10 percent range in percent impervious. Each 90- by 90-meter sample location was then overlaid with a 105-point, equilateral-triangle (hex) dot grid. Each point within the dot grid was then labeled as impervious or pervious based on the NAIP imagery. The percentage of dots identified as impervious served as the percent impervious value for that calibration sample. This was completed for approximately 300 samples within each moist study area.

The NLCD random sample calibration dataset was a simple random sample of pixels from the 2006 NLCD percent impervious product within each study area. The value from the NLCD percent impervious layer served as the training value for each point. A sample of 10,000 pixels was drawn for each study area.

Predictor Types

In order to better understand the ability of different predictor data types to properly predict percent impervious landcover, several sets of predictor data were tested. The predictor data types were chosen largely due to their success at predicting percent impervious landcover in previous studies (Chabaeva and others 2009; Ma and others 2010; Xu 2010). All predictors used in this study can be found in table 3. The predictor data were of two primary types—spectral and thermal. All spectral data were Landsat 5 Thematic Mapper (TM) data, while two different types of thermal data were tested. The Advanced Spaceborne Thermal Emission and Reflection Radiometer (ASTER) sensor aboard the Terra satellite has five thermal infrared bands ranging from 8.125 to 11.65 microns with a 90-meter spatial resolution. These five bands enable accurate surface emissivity estimates that result in enhanced temperature estimation (ASTER 2001). The ASTER-08 product depicts the modeled surface kinetic temperature on the kelvin scale (ASTER 2001). While the ASTER-08 product is the most accurate satellite-based depiction of land surface temperature, the pointable, tasked sensor provides inconsistent image extent and frequency, making ASTER impractical for use across a large area. In order to address this shortcoming of ASTER data, the Landsat 5 TM thermal infrared band was also tested and calibrated to the ASTER-08 data as outlined in Huang and others (2010b). The Landsat spectral data used in this study were reflectance corrected using the calibration and correction algorithms outlined in Huang and others (2010a). All Landsat TM data were resampled to a 90-meter spatial resolution and snapped to the ASTER-08 grid.

Once processed, the ASTER-08 thermal, Landsat thermal, and Landsat spectral data were tested as separate predictor data sets for each of the three study areas. Each set for each area contained multiple images from throughout a single growing season (table 3). This provided a more complete depiction of the variation in temperature and spectral reflectance across a growing season with respect to percent impervious landcover. This allows the modeling techniques to better identify patterns in the predictors across a growing season. The most complete set of spectral imagery across a single growing season was assembled over the Bend study area due to the quantity of cloud-free imagery.

Baltimore and Atlanta had greatly reduced image sets due to frequent cloud cover. The actual thermal temperature data were used as predictors within the thermal predictor sets, while spectral indices, as well as individual bands, were used as predictors for the spectral sets. In addition to Landsat TM bands 1, 2, 3, 4, 5, and 7, the Normalized Difference Vegetation Index (NDVI), Normalized Burn Ratio (NBR), Normalized Difference Moisture Index (NDMI), and the Vegetation Index Green (VIG) were used. (See table 4 for Landsat TM vegetation index algorithm details.) While highly correlated, each of these indices is sensitive to slightly different landcover types, and therefore could provide valuable information.

Table 3—Predictor rasters used in the analyses

City	Sensor	Image ID	Image Date	Season	Day/Night
Baltimore	Landsat	L5015033_03320060128	01/28/2006	Winter	Day
Baltimore	Landsat	L5015033_03320060418	04/18/2006	Spring	Day
Baltimore	Landsat	L5015033_03320060504	05/04/2006	Spring	Day
Baltimore	Landsat	L5015033_03320060824	08/24/2006	Summer	Day
Baltimore	Aster 08	AST_08_00303032004	03/03/2004	Winter	Day
Baltimore	Aster 08	AST_08_00304292001	04/29/2001	Winter	Night
Baltimore	Aster 08	AST_08_00308242003	08/24/2003	Summer	Day
Baltimore	Aster 08	AST_08_00310012005	10/01/2005	Summer	Night
Atlanta	Landsat	L5019037_03720060124	01/24/2006	Winter	Day
Atlanta	Landsat	L5019037_03720060414	04/14/2006	Spring	Day
Atlanta	Landsat	L5019037_03720060703	07/03/2006	Summer	Day
Atlanta	Landsat	L5019037_03720060804	08/04/2006	Summer	Day
Atlanta	Landsat	L5019037_03720060921	09/21/2006	Summer	Day
Atlanta	Aster 08	AST_08_00304052006	04/05/2006	Winter	Night
Atlanta	Aster 08	AST_08_00308232010	08/23/2010	Summer	Day
Bend	Landsat	L5045029_02920060420	04/20/2006	Spring	Day
Bend	Landsat	L5045029_02920060506	05/06/2006	Spring	Day
Bend	Landsat	L5045029_02920060607	06/07/2006	Spring	Day
Bend	Landsat	L5045029_02920060623	06/23/2006	Summer	Day
Bend	Landsat	L5045029_02920060725	07/25/2006	Summer	Day
Bend	Landsat	L5045029_02920060810	08/10/2006	Summer	Day
Bend	Landsat	L5045029_02920060826	08/26/2006	Summer	Day
Bend	Landsat	L5045029_02920060927	09/27/2006	Fall	Day
Bend	Landsat	L5045029_02920061013	10/13/2006	Fall	Day
Bend	Landsat	L5045029_02920061114	11/14/2006	Fall	Day

Table 4—Vegetation index algorithms for Landsat TM

Index Name	Index Abbreviation	Landsat TM Algorithm
Normalized Difference Vegetation Index	NDVI	(4-3)/(4+3)
Normalized Burn Ratio	NBR	(4-7)/(4+7)
Normalized Difference Moisture Index	NDMI	(4-5)/(4+5)
Vegetation Index Green	VIG	(2-3)/(2+3)

Direct Ecoregion Comparison Methods

Due to the adjacency of a moist and an arid ecoregion within the Pacific Northwest, a direct comparison was performed to better understand the impact of modeling distinct ecoregions with a single model as opposed to using different models for each ecoregion. This analysis was particularly beneficial since there is little knowledge of the impact of varying ecoregions on percent impervious models. The study area was the intersection of the level 1 Environmental Protection Agency (EPA) ecoregions (Bibeau 1997) and MODIS Aqua swath H9, V4. The same set of model types used in Baltimore, Altanta, and Bend were used in this analysis. The models were tested on MODIS 8-day composite spectral (MYD09Q1) and thermal (MOD11A2) data from the Aqua platform, using NLCD percent impervious values to calibrate all models. A stratified random sample was necessary in order to adequately sample the rare urban areas within the arid ecoregion. The urban stratification was created by thresholding the NLCD percent impervious landcover product at 75% impervious. The first modeling step trained the model using all calibration data, which spanned both ecoregions. The model was then applied to the entire study region. The next step calibrated the model using only calibration data from the arid ecoregion and then applied the calibrated model to the entire study region. The final step calibrated the model using only calibration data from the moist ecoregion and then applied the model to the entire study region.

Validation Methods

Due to budget constraints, an independent validation was not conducted. A 10-fold cross validation and bootstrap resampling validation was implemented to serve as a surrogate for an independent validation. The primary metrics used from the 10-fold cross validation and bootstrap resampling validation are the root mean squared error (RMSE) :

$$RMSE = \sqrt{\frac{1}{n}\sum_{j=1}^{n}\left(y_j - \hat{y}_j\right)^2}$$

and the mean absolute error (MAE):

$$MAE = \frac{1}{n}\sum_{j=1}^{n}\left|y_j - \hat{y}_j\right|$$

n = number of samples

y_j = modeled value

$\hat{y}_j$ = observed value

While RMSE is a standard metric of model efficacy, it is highly leveraged by outliers. MAE is not influenced in the same way as RMSE by outliers. While often very similar, RMSE and MAE do provide insight into how the model may deal with outliers versus the larger proportion of the population.

Results

Due to the combinatorial nature of the research design, the results from each stage of the study will be summarized in the context of the best result from the remaining phases. The overall results indicate that the best combination of methods for modeling percent impervious landcover is to apply individual models across individual ecoregion types, using a Cubist model within moist ecoregions, and either a random forests or Cubist model within arid regions depending on the priority placed on model run time. The best method for training a model is to use a sample of existing modeled data, while the best predictors are Landsat spectral data. Examples of results from each study area using different modeling methods can be seen in figures 2, 3, and 4.

Model Methods

Testing three different model types provided a more complete picture of the strengths and weaknesses of different model types. Models were compared both by the error within the results and the run times. Each of these metrics of model proficiency provides useful information for choosing the proper model. In general, Cubist had the fastest run times (figure 5). This is due to its relative computational simplicity. All models had similar error rates within a given ecoregion (figure 6). If the model run time is a high priority, Cubist proved to provide the best product. The support vector machine did provide a visually superior product within the moist ecoregions, but had significantly longer run times. The output from random forests within the moist ecoregions was quantitatively on par with the support vector machine output (figure 6, appendix A), but was visually noisy. All three modeling methods excelled in the Bend study area. Much of the noise that was present in the moist ecoregion random forests product was absent in the arid ecoregion product. While the number of study areas tested was limited, these results suggest that the Cubist modeling technique is sufficient in both moist and arid ecoregions.

Calibration Method

Each of the tested calibration methods has apparent advantages for an operational percent impervious landcover project. Creating the photo-interpreted calibration dataset was time consuming and manually intensive. Sampling an existing product takes seconds to complete. The results indicate that overall, a larger sample of the existing NLCD percent impervious landcover product results in a more effective model than a relatively small photo-interpreted calibration dataset (figure 7). This is likely because the photo-interpreted calibration dataset did not sufficiently sample the landscape. The sample was a stratified

random sample, with sample sizes carefully chosen as a function of optimizing the variance sampled of the distribution of the individual pixel values within the stratum for the study area. Despite these careful measures, a simple random sample of many NLCD percent impervious landcover pixels proved to be the most effective method. This is indicated in both moist study areas, with all modeling methods (figure 7, appendix 1). While these results do indicate that using the existing NLCD percent impervious landcover product is effective, it should not be inferred that all existing related products would outperform photo-interpreted calibration datasets.

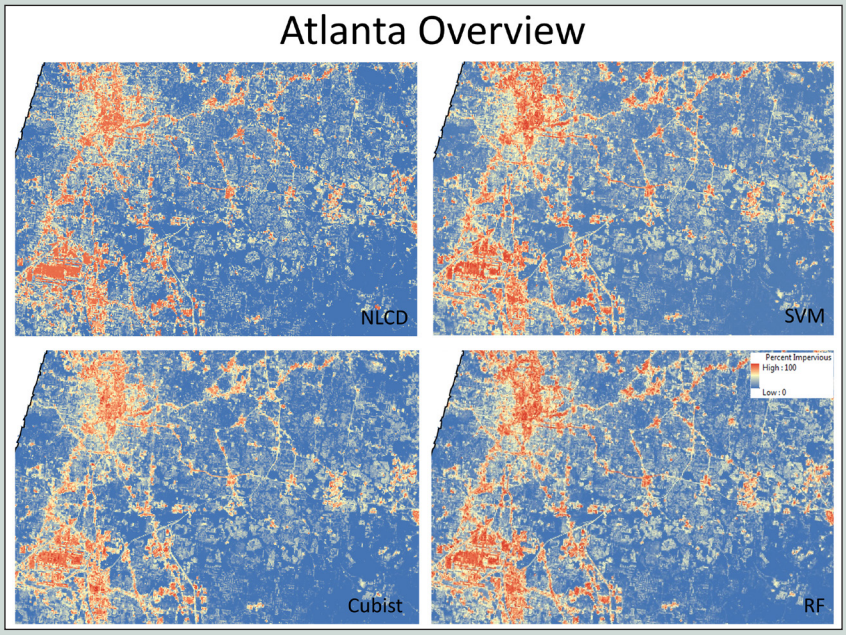

Figure 2—Comparison of the outputs of the three modeling methods to the NLCD percent impervious product. Visually, the differences are largely minimal within the Atlanta study area.

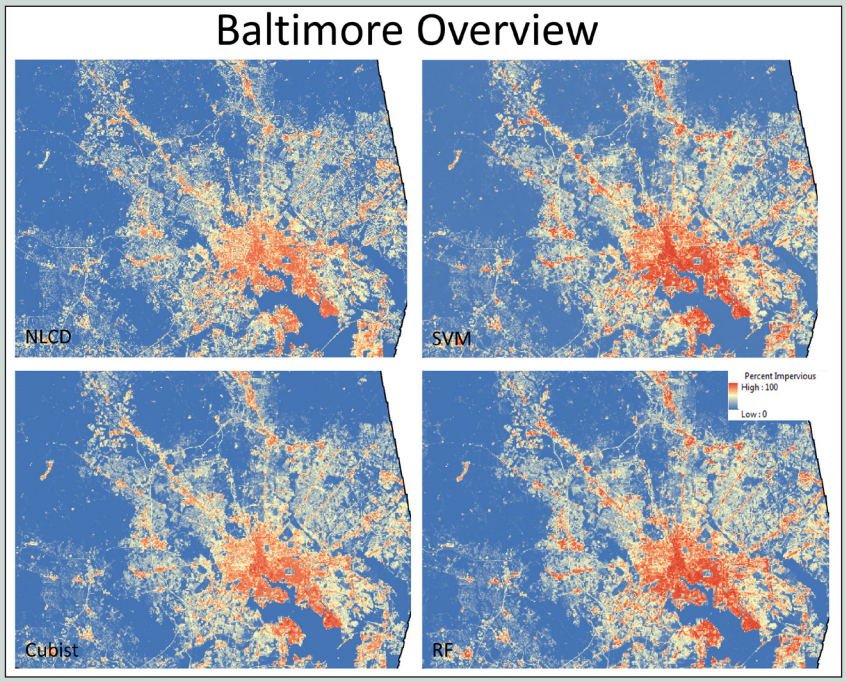

Figure 3—Comparison of the outputs of the three modeling methods to the NLCD percent impervious product. Visually, the differences are largely minimal within the Baltimore study area.

Predictor Data Type

Identifying optimal predictor data is one of the primary considerations when creating a model. The results from this study indicate that the efficacy of different predictor data types varies between ecoregions (figure 8, appendix 1). This study tested two thermal and one spectral predictor data types. Both ASTER and Landsat TM thermal data products produced qualitatively proficient models. Landsat spectral data outperformed Landsat thermal data at predicting percent impervious landcover within moist and arid areas. The robustness of the spectral data at predicting percent impervious landcover across different ecoregions suggests that spectral data would be favorable to thermal data.

Direct Ecoregion Comparison

The results from the ecoregion comparison illustrate the effects of separating analysis areas by ecoregions (figure 9). The results are presented both visually and quantitatively in figures 9 and 10, respectively. Visually, the unseparated output indicates that the model works well in the moist ecoregion (western half), while the urban areas within the arid ecoregion (eastern half) are often under-predicted (figure 9). When only arid ecoregion calibration data are used, this error is reduced, but still present. When only moist ecoregion calibration data are used, there is minimal difference to the output within the moist ecoregion, while the visual error within the arid ecoregion is significantly increased. Many of these differences are not apparent in the RMSE and MAE

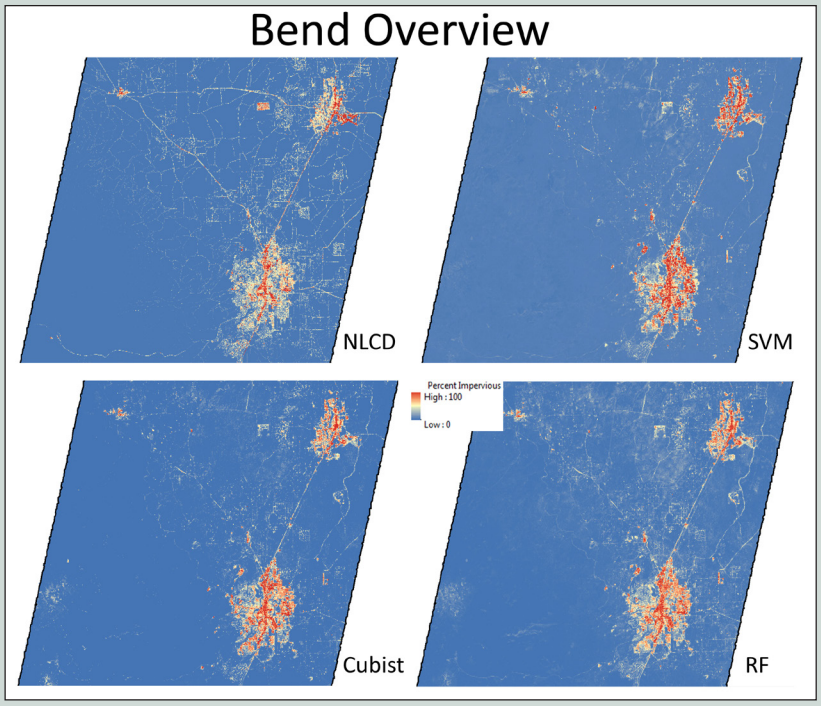

Figure 4—Comparison of the outputs of the three modeling methods to the NLCD percent impervious product. Visually, the differences largely occur within the rural upland areas in the center left section of the images. All models over-predict in these areas. All modeled products lack the roads that appear within the NLCD product. Many of these roads are no longer in existence, or are unpaved. They do not appear in the modeled product because they are largely pervious and no road layer was used in the modeling process.

(figure 10). The relatively low error rate within the arid ecoregion is likely due to the large portion of the landscape that has a low percent impervious. These areas are generally easier to model than the areas with moderate percent impervious landcover found in greater abundance within the moist ecoregion. One potential difficulty was observed in the transition zone in north central Washington State (figure 9). There the transition zone between ecoregions was inaccurately modeled. By their very nature, transition zones will always cause difficulty for models. It is clear from these results that separating calibration data by ecoregion has a profound impact on model output. It remains unclear how much the results are being leveraged by the relative proportions of human-influenced and natural landcover within the given ecoregion.

Discussion

This study begins to answer many necessary questions to effectively model percent impervious landcover on a continental scale on an annual basis. While the existing literature does provide extensive insight regarding model efficacy, and predictor data selection, the knowledge gap in understanding the variability of percent impervious landcover modeling is one that merits continued investigation. The results of this study indicate that all modeling methods used have their place on an operational percent impervious landcover modeling process. While support vector machines did prove to be a robust modeling method across both ecoregions, it is far more computationally intensive than random forests or Cubist. Random forests is very effective at finding patterns in complex data, and does provide a quick, unbiased idea of model efficacy. Considering proficiency for the given model runtime, Cubist is the model of choice in both ecoregions.

While different modeling methods were tested in this study, many of the parameters that may influence the efficacy of these models were not fully explored. Further insight into the impacts of various modeling parameters could potentially enhance the modeling process.

Although the results indicate that existing percent impervious landcover data is the most effective model calibration method, using a modeled product to calibrate a model raises many additional questions. This cyclical approach permits the output to inherit bias and inaccuracies of the original model output (Nowak and Greenfield 2010; Raciti and others 2012; Zheng and others 2012). If a model failed in a certain instance previously, any subsequent model is highly unlikely to correct such an error. Additionally, any modeled percent impervious landcover product represents the percent impervious landcover at a point in time. Since the NLCD percent impervious landcover product is updated every 5 years, any subsequent change that occurs would be represented by a pre-change percent impervious landcover value. Omitting such changed locations from the sampled population of values is necessary, but requires a preliminary change analysis to ensure that only unchanged pixels are included in the sample population. This introduces bias in the sample population, since areas adjacent to areas that are already highly impermeable are more likely to undergo development. Nevertheless, the inclusion of changed pixels in the sampled population introduces far more model confusion. While it is understood that a nationwide rapid-return product (< 2 year refresh) would require some

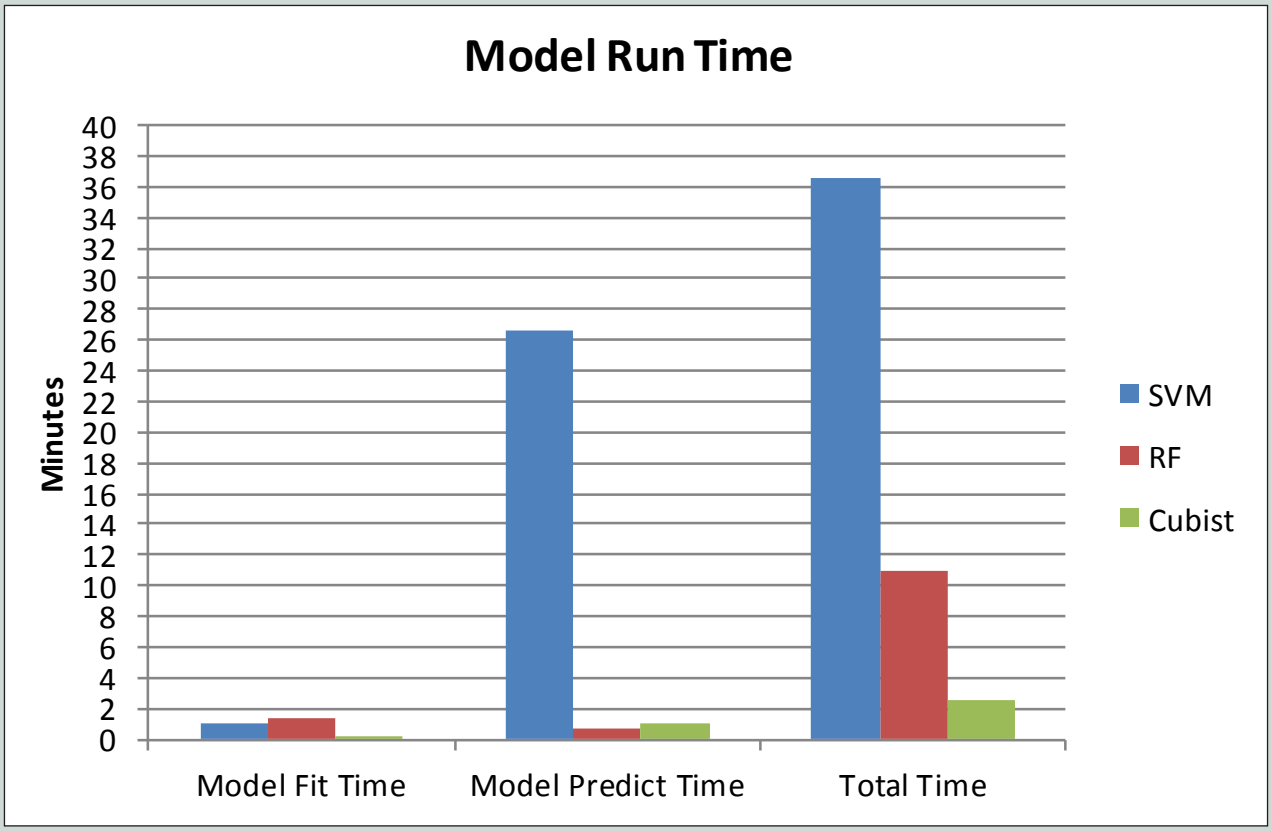

Figure 5—Model run time for each modeling method in the Baltimore study area using NLCD calibration data. The individual components of the modeling process are presented, along with the total modeling time. The total time includes the model fit time, model predict time, and time to write the raster. Cubist is the quickest, while support vector machines prove to be the most computationally intensive.

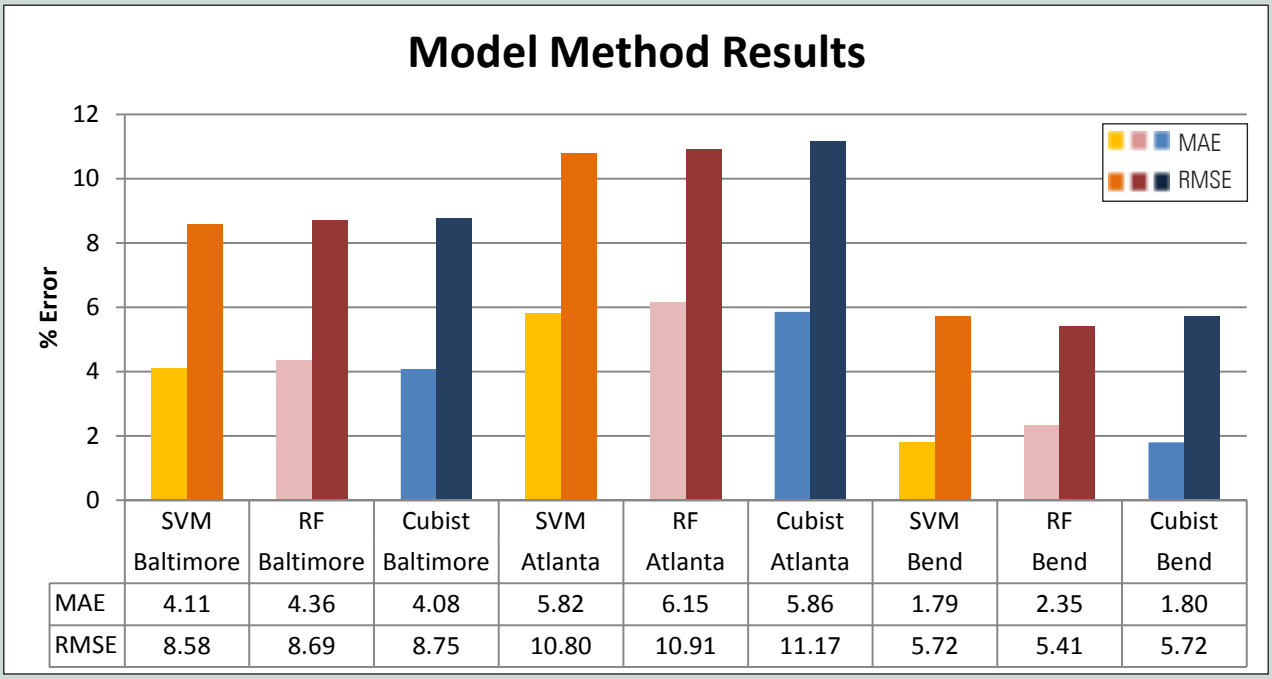

	SVM Baltimore	RF Baltimore	Cubist Baltimore	SVM Atlanta	RF Atlanta	Cubist Atlanta	SVM Bend	RF Bend	Cubist Bend
MAE	4.11	4.36	4.08	5.82	6.15	5.86	1.79	2.35	1.80
RMSE	8.58	8.69	8.75	10.80	10.91	11.17	5.72	5.41	5.72

Figure 6—MAE and RMSE values of the best predictor type and calibration method across the different modeling methods.

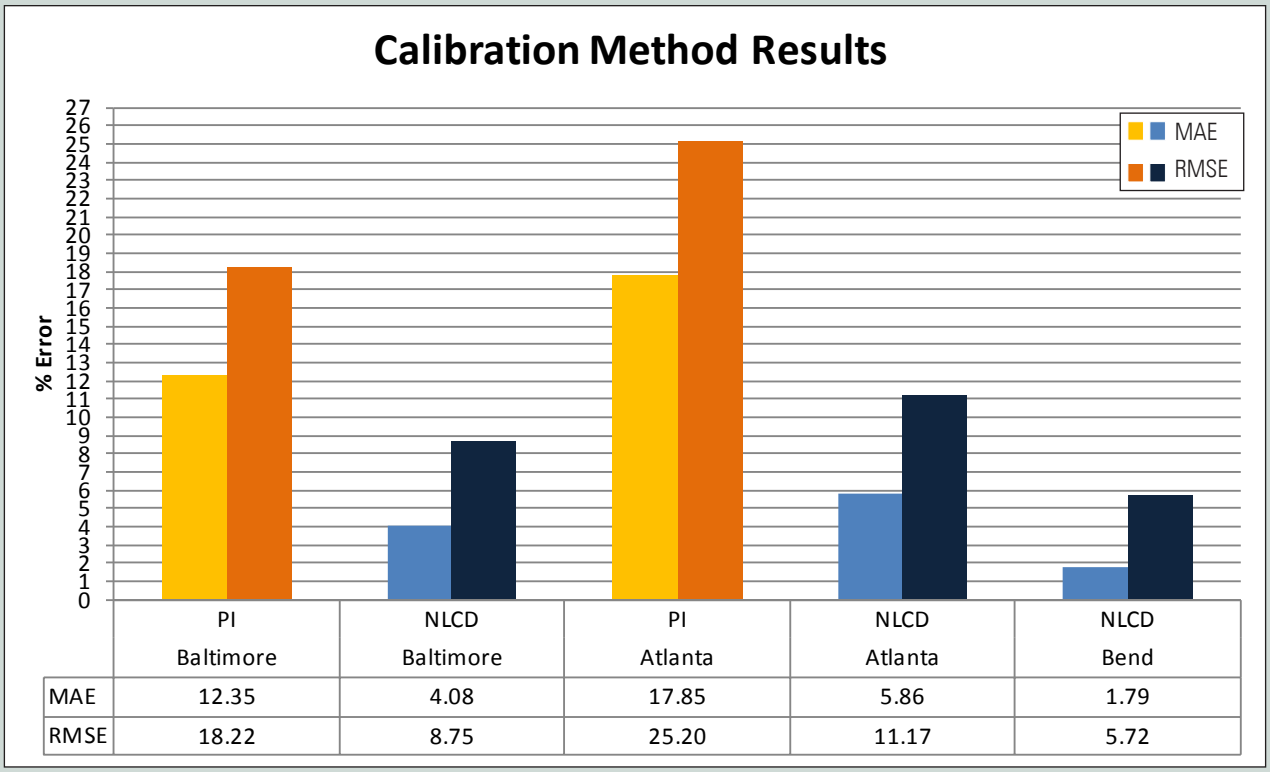

Figure 7—MAE and RMSE values of the best modeling method and predictor type across the different calibration methods.

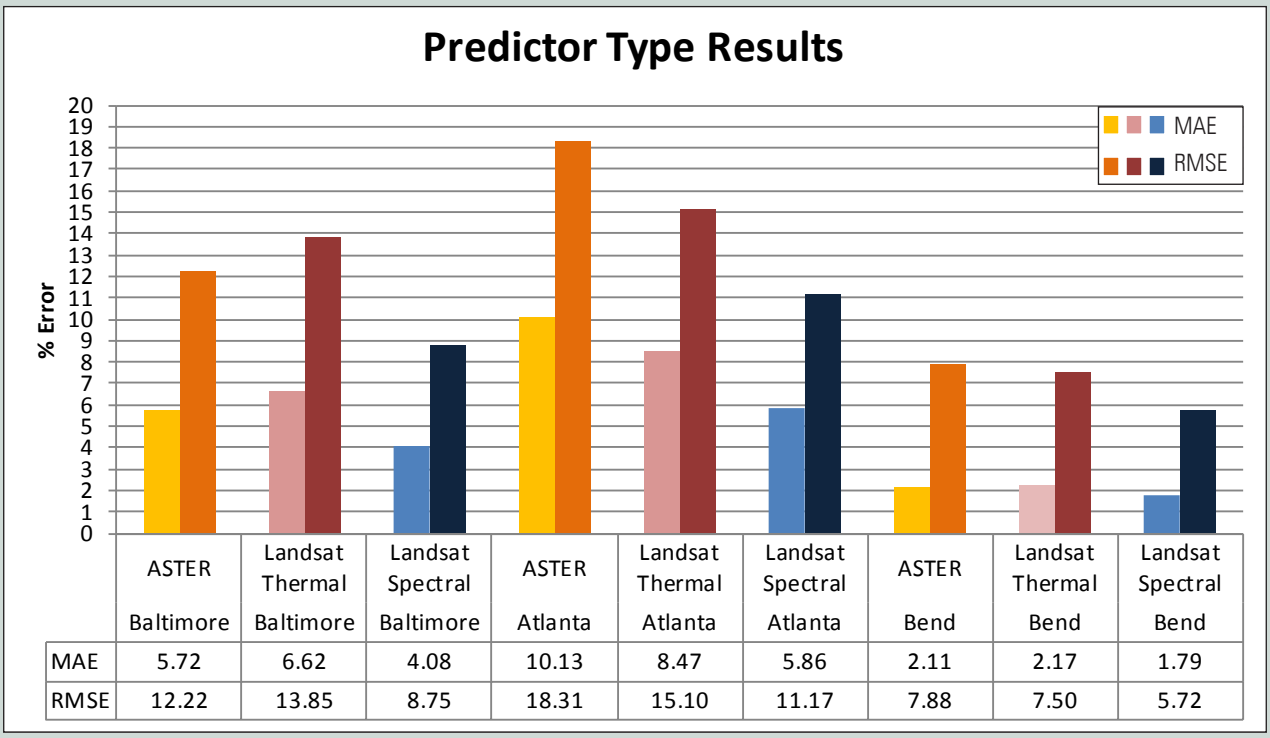

Figure 8—MAE and RMSE values of the best modeling and calibration method across the different predictor types.

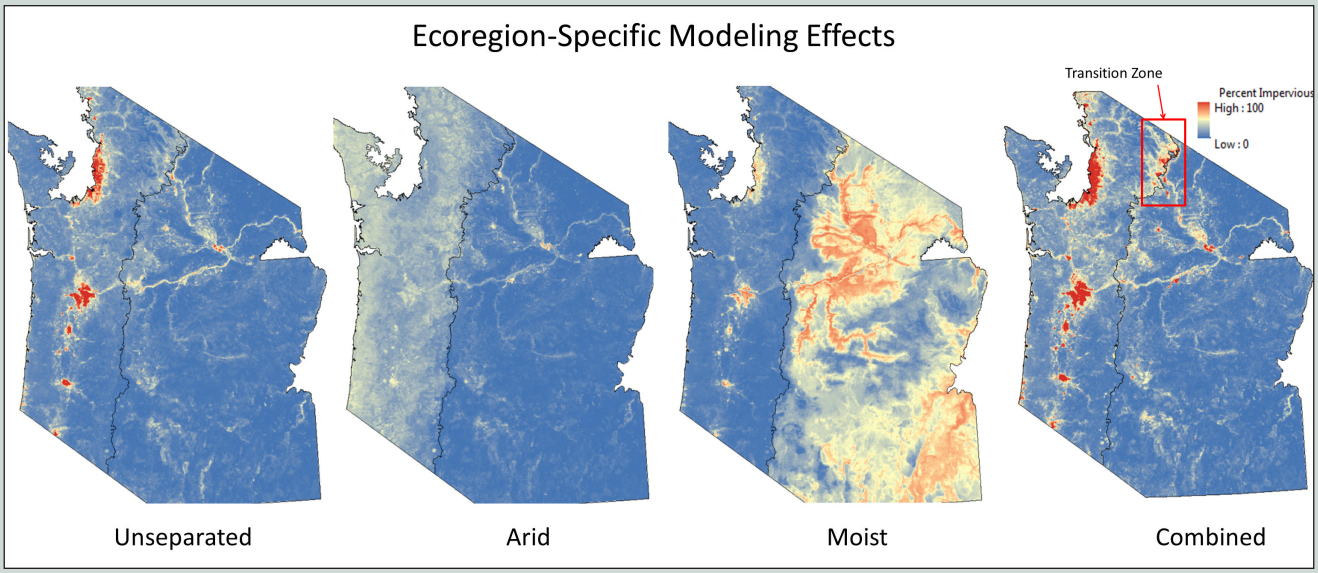

Figure 9—Example outputs from the ecoregion comparison study. The unseparated image is the result of using training data from both the arid and moist ecoregions, while the arid and moist images are produced using calibration values from their respective ecoregions. The combined image is the mosaic of the moist and arid region outputs from the respective ecoregion. The impacts of using calibration data from each respective ecoregion are apparent. The unseparated output tends to under-predict percent impervious in the arid ecoregion, while the combined output tends to slightly over-predict percent impervious in the arid area.

automation of model calibration data acquisition, due to these difficulties, it is recommended that a more comprehensive review of model calibration methods is performed.

While individual predictor data types were tested, an understanding of the utility of using multiple predictor data types in unison was not investigated due to the combinatorial nature of such an investigation. It is possible that model efficacy could be enhanced by using multiple predictor data types to model percent impervious landcover.

Although separating models by ecoregion proved important, moisture levels are highly variable across time and space. Ecoregions may or may not be the best method for stratifying the landscape. Additionally, many individual areas in transition zones may prove difficult to model as one zone type or the other. A better understanding of the optimal method for stratifying the landscape would increase model efficacy.

Addressing these issues will help ensure that any annually modeled percent impervious landcover product is modeled in the most effective and efficient manner with the current state of the art. If these issues remain unaddressed, the quality of any product and change detection ability may be compromised.

References

ASTER. 2001. ASTER Higher-Level Product User Guide. Version 2.0. JPL D-20062. Jet Propulsion Laboratory 80 p. http://asterweb.jpl.nasa.gov/content/03_data/04_Documents/ASTERHigherLevelUserGuideVer2May01.pdf (May 2, 2013).

Bibeau, D. 1997. Ecological regions of North America—toward a common perspective. Montreal, Canada: Legal Deposit–Bibliothèque Nationale du Québec. 71 p.

Breiman, L. 2001. Random forests. Machine Learning. 45(1): 5-32.

Chabaeva, A.; Civco, D.L.; Hurd, J.D. 2009. Assessment of impervious surface estimation techniques. Journal of Hydrologic Engineering. 14(4): 377-387.

Cohen, B. 2004. Urban growth in developing countries: a review of current trends and a caution regarding existing forecasts. World Development. 32(1): 23-51.

Cohen, B. 2006. Urbanization in developing countries: Current trends, future projections, and key challenges for sustainability. Technology in Society. 28: 63-80.

Cortes, C.; Vapnik, V.N. 1995. Support-vector networks. Machine Learning. 20(3): 273-297.

Fry, J.; Xian, G.; Jin, S.; Dewitz, J.; Homer, C.; Yang, L.; Barnes, C.; Herold, N.; Wickham, J. 2011. Completion of the 2006 National Land Cover Database for the conterminous United States. Photogrammetric Engineering & Remote Sensing. 77(9): 858-864.

Ghimire, B.; Rogan, J.; Galiano, V.R.; Panday, P.; Neeti, N. 2012. An evaluation of bagging, boosting, and Random Forests for land-cover classification in Cape Cod, Massachusetts, USA. GIScience and Remote Sensing. 49(5): 623-643.

Ghosh, T.; Powell, R.L.; Elvidge, C.D.; Baugh, K.E.; Sutton, P.C.; Anderson, S. 2010. Shedding light on a global distribution of economic activity. The Open Geography Journal. 3(1): 148-161.

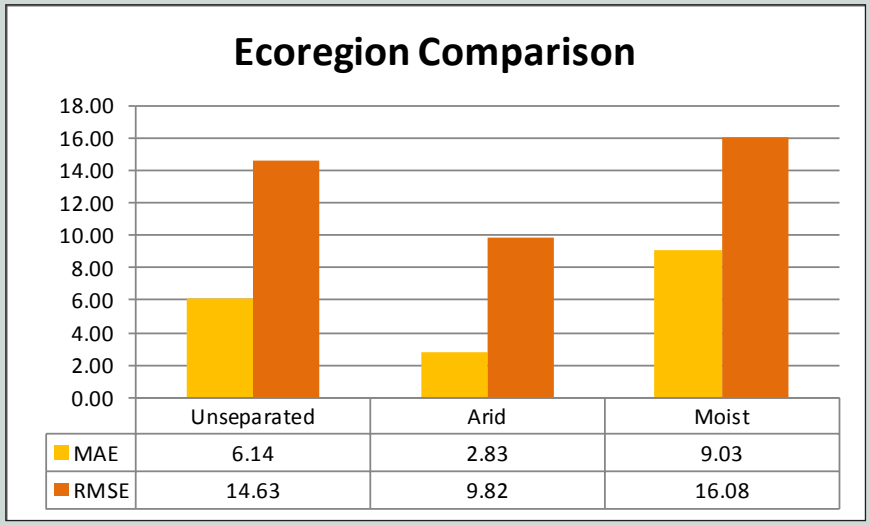

Figure 10—MAE and RMSE from a 10-fold cross validation of the ecoregion comparison results from the random forests model using MODIS spectral data.

Huang, C.; Goward, S.N.; Masek, J.G.; Thomas, N.; Zhu, Z.; Vogelmann, J.E. 2010a. An automated approach for reconstructing recent forest disturbance history using dense Landsat time series stacks. Remote Sensing of Environment. 114(1): 183-198.

Huang, C; Song, K.; Kim, S.; Townshend, J.R.G.; Davis, P. ; Masek, J.G.; Goward, S.N. 2008. Use of dark object concept and support vector machine to automate forest cover change analysis. Remote Sens. Environ. 112: 970–985

Huang, C.; Thomas, N.; Goward, S.N.; Masek, J.G.; Zhu, Z.; Townshend, J.R.G.; Vogelmann, J.E. 2010b. Automated masking of cloud and cloud shadow for forest change analysis using Landsat images. International Journal of Remote Sensing. 31(20): 5449-5464.

Ma, Y.; Kuang, Y.; Huang, N. 2010. Coupling urbanization analyses for studying urban thermal environment and its interplay with biophysical parameters based on TM/ETM+ imagery. International Journal of Applied Earth Observation and Geoinformation. 12(2): 110-118.

Mieszkowski, P.; Mills, E.S. 1993. The causes of metropolitan suburbanization. Journal of Economic Perspectives. 7(3): 135-147.

Nowak, D.J.; Greenfield, E.J. 2012. Tree and impervious cover in the United States. Landscape and Urban Planning. 107: 21-30.

R Development Core Team. 2010. R: A language and environment for statistical computing. R Foundation for Statistical Computing, Vienna, Austria. http://www.R-project.org (January 31, 2013).

Raciti, S.; Hutyra, L.; Rao, P.; Finzi, A. 2012. Inconsistent definitions of "urban" result in different conclusions about the size of urban carbon and nitrogen stocks. Ecological Applications. 22(3): 1015-1035.

Walton, J.T. 2008. Subpixel urban land cover estimation: comparing Cubist, Random Forests, and support vector regression. Photogrammetric Engineering & Remote Sensing. 74(10): 1213-1222.

Wrigley, E.A. 1985. Urban growth and agricultural change: England and the continent in the early modern period. Journal of Interdisciplinary History. 15(4): 683-728.

Xian, G.; Homer, C.; Dewitz, J.; Fry, J.; Hossain, N.; Wickham, J. 2011. The change of impervious surface area between 2001 and 2006 in the conterminous United States. Photogrammetric Engineering & Remote Sensing. 77(8): 758-762.

Xu, H. 2010. Analysis of impervious surface and its impact on urban heat environment using the Normalized Difference Impervious Surface Index (NDISI). Photogrammetric Engineering & Remote Sensing. 76(5): 557-565.

Zheng, D.; Heath, L.S.; Ducey, M.J. 2012. Potential overestimation of carbon sequestration in the forested wildland-urban interface in northern New England. Journal of Forestry. 110(2): 105-111.

For additional information, contact:

Haans Fisk, RSEAT Program Leader
Remote Sensing Evaluation,
Applications & Training
Remote Sensing Applications Center
2222 West 2300 South
Salt Lake City, UT 84119

phone: (801) 975-3750
e-mail: mailroom_wo_rsac@fs.fed.us

This publication can be downloaded from the RSAC Web site: http://fsweb.rsac.fs.fed.us

Non-Discrimination Policy

The U.S. Department of Agriculture (USDA) prohibits discrimination against its customers, employees, and applicants for employment on the bases of race, color, national origin, age, disability, sex, gender identity, religion, reprisal, and where applicable, political beliefs, marital status, familial or parental status, sexual orientation, or all or part of an individual's income is derived from any public assistance program, or protected genetic information in employment or in any program or activity conducted or funded by the Department. (Not all prohibited bases will apply to all programs and/or employment activities.)

To File an Employment Complaint

If you wish to file an employment complaint, you must contact your agency's EEO Counselor (PDF) within 45 days of the date of the alleged discriminatory act, event, or in the case of a personnel action. Additional information can be found online at http://www.ascr.usda.gov/complaint_filing_file.html.

To File a Program Complaint

If you wish to file a Civil Rights program complaint of discrimination, complete the USDA Program Discrimination Complaint Form (PDF), found online at http://www.ascr.usda.gov/complaint_filing_cust.html, or at any USDA office, or call (866) 632-9992 to request the form. You may also write a letter containing all of the information requested in the form. Send your completed complaint form or letter to us by mail at U.S. Department of Agriculture, Director, Office of Adjudication, 1400 Independence Avenue, S.W., Washington, D.C. 20250-9410, by fax (202) 690-7442 or email at program.intake@usda.gov.

Persons with Disabilities

Individuals who are deaf, hard of hearing or have speech disabilities and you wish to file either an EEO or program complaint please contact USDA through the Federal Relay Service at (800) 877-8339 or (800) 845-6136 (in Spanish).

Persons with disabilities who wish to file a program complaint, please see information above on how to contact us by mail directly or by email. If you require alternative means of communication for program information (e.g., Braille, large print, audiotape, etc.) please contact USDA's TARGET Center at (202) 720-2600 (voice and TDD).

Appendix A: Comprehensive List of Analysis Results

MAE, RMSE, R-squared and run time values from all combinations of methods tested across the three study areas. MAE, RMSE, and R-squared values were calculated using a 10-fold cross validation. The best combination of calibration method, predictor type, and model type by minimum MAE is bolded. It should be noted that the MAE from the Cubist model in Bend and Atlanta is very close to the MAE of SVM.

Table A-1—Comprehensive list of analysis results

City	Calibration Method	Predictors	Model Method	MAE	RMSE	R2	Run Time (Minutes)
Baltimore	PI	ASTER 08	svm	14.73	21.36	0.515	1.92
Baltimore	PI	ASTER 08	rf	16.49	22.23	0.464	0.73
Baltimore	PI	ASTER 08	cubist	17.66	26.04	0.354	1.08
Baltimore	NLCD	ASTER 08	svm	5.87	12.21	0.723	39.58
Baltimore	NLCD	ASTER 08	rf	6.46	12.16	0.722	9.21
Baltimore	NLCD	ASTER 08	cubist	5.72	12.22	0.724	1.47
Baltimore	PI	Landsat TM Thermal	svm	15.92	22.06	0.484	1.92
Baltimore	PI	Landsat TM Thermal	rf	16.54	21.65	0.489	0.84
Baltimore	PI	Landsat TM Thermal	cubist	19.20	26.57	0.335	1.52
Baltimore	NLCD	Landsat TM Thermal	svm	6.64	13.50	0.663	41.62
Baltimore	NLCD	Landsat TM Thermal	rf	7.40	13.36	0.664	11.15
Baltimore	NLCD	Landsat TM Thermal	cubist	6.62	13.85	0.649	2.58
Baltimore	PI	Landsat TM Spectral	svm	12.25	17.94	0.654	1.93
Baltimore	PI	Landsat TM Spectral	rf	13.39	18.25	0.637	0.77
Baltimore	PI	Landsat TM Spectral	cubist	12.35	18.22	0.641	1.30
Baltimore	NLCD	Landsat TM Spectral	svm	4.11	8.58	0.862	36.59
Baltimore	NLCD	Landsat TM Spectral	rf	4.36	8.69	0.858	10.91
Baltimore	**NLCD**	**Landsat TM Spectral**	**cubist**	**4.08**	**8.75**	**0.857**	**2.60**
Atlanta	PI	ASTER 08	svm	22.04	30.36	0.200	1.52
Atlanta	PI	ASTER 08	rf	24.06	30.54	0.153	0.81
Atlanta	PI	ASTER 08	cubist	22.10	29.73	0.205	0.73
Atlanta	NLCD	ASTER 08	svm	10.61	18.64	0.386	38.04
Atlanta	NLCD	ASTER 08	rf	11.60	18.32	0.384	7.12
Atlanta	NLCD	ASTER 08	cubist	10.13	18.31	0.416	1.13

(Continued on next page)

Table A-1—Comprehensive list of analysis results ***(Continued from previous page)***

City	Calibration Method	Predictors	Model Method	MAE	RMSE	R2	Run Time (Minutes)
Atlanta	PI	Landsat TM Thermal	svm	20.51	28.71	0.262	1.59
Atlanta	PI	Landsat TM Thermal	rf	22.38	28.59	0.228	0.90
Atlanta	PI	Landsat TM Thermal	cubist	21.05	29.03	0.234	1.38
Atlanta	NLCD	Landsat TM Thermal	svm	8.24	14.68	0.611	38.92
Atlanta	NLCD	Landsat TM Thermal	rf	9.12	14.60	0.605	14.43
Atlanta	NLCD	Landsat TM Thermal	cubist	8.47	15.10	0.589	3.16
Atlanta	PI	Landsat TM Spectral	svm	17.77	26.35	0.366	1.57
Atlanta	PI	Landsat TM Spectral	rf	18.81	25.35	0.387	0.94
Atlanta	PI	Landsat TM Spectral	cubist	17.85	25.20	0.406	1.29
Atlanta	NLCD	Landsat TM Spectral	svm	5.82	10.80	0.787	37.28
Atlanta	NLCD	Landsat TM Spectral	rf	6.15	10.91	0.779	13.18
Atlanta	**NLCD**	**Landsat TM Spectral**	**cubist**	**5.86**	**11.17**	**0.772**	**2.88**
Bend	NLCD	ASTER 08	svm	2.26	7.81	0.003	13.47
Bend	NLCD	ASTER 08	rf	3.55	7.83	0.020	2.62
Bend	NLCD	ASTER 08	cubist	2.11	7.88	0.003	0.81
Bend	NLCD	Landsat TM Thermal	svm	2.17	7.50	0.246	14.49
Bend	NLCD	Landsat TM Thermal	rf	3.04	6.62	0.241	4.93
Bend	NLCD	Landsat TM Thermal	cubist	2.21	7.01	0.180	3.04
Bend	**NLCD**	**Landsat TM Spectral**	**svm**	**1.79**	**5.72**	**0.476**	**14.96**
Bend	NLCD	Landsat TM Spectral	rf	2.35	5.41	0.493	4.37
Bend	NLCD	Landsat TM Spectral	cubist	1.80	5.72	0.445	2.67

Note: The best combination of calibration method, predictor type, and model type by minimum MAE is bolded. It should be noted that the MAE from the Cubist model in Bend and Atlanta is very close to the MAE of SVM.